

# Passive WiFi CSI Sensing Based Machine Learning Framework for COVID-Safe Occupancy Monitoring

Aryan Sharma<sup>†</sup>, Junye Li<sup>†</sup>, Deepak Mishra<sup>†</sup>, Gustavo Batista<sup>\*</sup>, Aruna Seneviratne<sup>†</sup>

School of Electrical Engineering and Telecommunications, University of New South Wales, Sydney, NSW 2052, Australia<sup>†</sup>

School of Computer Science and Engineering, University of New South Wales, Sydney, NSW 2052, Australia<sup>\*</sup>

Emails: {aryan.sharma, junye.li, d.mishra, g.batista, a.seneviratne}@unsw.edu.au

**Abstract**—The COVID-19 pandemic requires social distancing to prevent transmission of the virus. Monitoring social distancing is difficult and expensive, especially in “travel corridors” such as elevators and commercial spaces. This paper describes a low-cost and non-intrusive method to monitor social distancing within a given space, using Channel State Information (CSI) from passive WiFi sensing. By exploiting the frequency selective behaviour of CSI with a cubic SVM classifier, we count the number of people in an elevator with an accuracy of 92%, and count the occupancy of an office to 97%. As opposed to using a multi-class counting approach, this paper aggregates CSI for the occupancies below and above a COVID-Safe limit. We show that this binary classification approach to the COVID safe decision problem has similar or better accuracy outcomes with much lower computational complexity, allowing for real-world implementation on IoT embedded devices. Robustness and scalability is demonstrated through experimental validation in practical scenarios with varying occupants, different environment settings and interference from other WiFi devices.

## I. INTRODUCTION

Due to COVID-19, the world has seen tremendous restrictions placed on the manner in which people may navigate public spaces. Health Authorities identified physical distancing as one effective measure that can be taken to reduce the spread of the virus, and authorities in a majority of the countries have mandated social distancing. The recommendation is for individuals to maintain a physical separation of at least 1.5m and public spaces to have limited occupancy, namely 1 person per 4 square metres [1]. Numerous technological solutions have been proposed to help organisations promote and monitor the adherence to the social distancing recommendations [2] [3] [4] [5]. The majority of these proposed solutions require the users wearing a “tag”, using/having an active mobile device such as a smartphone, or the organisations installing special equipment such as cameras or microphones. These solutions can introduce privacy issues or be expensive. In this paper, we present a WiFi sensing approach that can alert people of social distancing breaches, which does not violate their privacy and is cost effective. A number of recent studies show that WiFi can be used to track patrons in a physical environment, and we hope to extend this to a COVID context.

We make the following contributions:

- Demonstrating that it is possible to make the necessary CSI measurements using only 3 low cost commercial

off-the-shelf devices (Raspberry Pi) and open source software (Nexmon [6]);

- Proposing a new machine learning model with robust features based on the unique response of Orthogonal Frequency Division Multiplexing (OFDM) subcarriers, exploiting the frequency-selective behavior of the measured CSI to accurately count the number of occupants;
- Empirically demonstrating the viability of the proposed system in a controlled Elevator environment. Our system can detect if the COVID safe limit is violated in the elevator to an accuracy of 97%.
- Validation in the practical scenario of an office, where our system achieves a robust 97% counting accuracy despite interference from user WiFi devices and movement of the occupants.

## II. RELATED WORK

In this section, we introduce existing architectures for WiFi sensing, the data used as well as signal processing and machine learning methods. In all cases, WiFi sensing involves analysing the variations in a received signal to understand the environment in the signal path [7]. Although a number of studies have shown the possibility of using RSSI to predict activities such as walking, squatting, and running, these systems are susceptible to sporadic noise in the channel, and has limited applicability, especially when there are more than one person involved [8]. Recently, studies have shown that CSI, which provides indication of the degree to which a signal was attenuated and delayed by the signal path (channel), can be used to detect humans and their activities more robustly [9] [10].

### A. CSI Based Detection

Diverse approaches have been taken to mitigate the measurement noise in CSI, including low-pass techniques [11] [12] and dimensionality reduction such as Principle Component Analysis (PCA) [13] [9]. Furthermore, existing work has found CSI collection to contain outliers due to WiFi transmission characteristics, and hence outlier removal techniques such as Hampel Filter have been successful [7].

Following data cleansing, several studies have found artifacts of human activity or objects manifested within CSI data [9] [10]. Static objects in the wireless signal path uniquely affect the CSI of different OFDM subcarriers, and this can be exploited for profiling objects in the channel [14] [15].

In particular, one study found the skewness and entropy across OFDM subcarriers to be a highly relevant feature for classifying static objects [15]. These features have yet to be exploited for *counting* humans.

### B. Counting Humans and Machine Learning

More specific to our cause, *DeepCount* [16] used CSI to count crowd sizes. This study proposed that conventional statistical features were unable provide accurate counting from supervised learning. Instead, they opted to extract deep features from CSI with a deep learning classification algorithm and were able to count up to 5 people to an accuracy of 85%. Here, we find a potential for improvement. There is potential for frequency-based features, used already to classify objects [14], to be utilised for more robust counting of occupants in the channel. Furthermore, there is a need for a practical application of such a system with demonstrated results in a changing environment such as an elevator with opening and closing doors. There is scope for improved classification algorithms to be used for better accuracies and lower complexity. In literature, the performance of Support Vector Machines (SVM), Naive Bayesian Classifiers, Random Forest Modeling, and Gaussian Mixture Models for classifying CSI have been compared [12] [9]. SVM is a supervised classification approach which determines the best hyperplane with which to divide a dataset into defined classes. Of the studied classifiers, SVM is favourable as it offered the best accuracy outcomes for minimal computational cost [12].

## III. SYSTEM DESCRIPTION

In this section we describe the foundations behind WiFi CSI-based human counting. We describe CSI and the device architecture with which it can be captured.

### A. CSI Sensing Model

All wireless signals propagating from a transmitter (Tx) to a receiver (Rx) are affected by the wireless channel. This can be represented by the transmission model [17]:

$$Y(f, t) = H(f, t)X(f, t) + N(f, t) \quad (1)$$

where any time instant  $t$  and carrier frequency  $f$ ,  $Y(f, t)$  is the received wireless signal,  $X(f, t)$  is the transmitted signal and  $H(f, t)$  represents the manner in which the channel affects the transmitted signal. The noise  $N(f, t)$  is sometimes modelled as Gaussian noise across all subcarriers. 802.11n and subsequent wireless protocols employ OFDM, whereby data is modulated onto many different frequency waves known as *subcarriers*. Hence, this transmission occurs over 56 subcarrier waves with varying frequencies spanning the 20MHz channel. We can obtain the CSI,  $H(f, t)$ , for each of these subcarriers with frequency  $f$ . Essentially, we obtain a complex value at any time  $t$  which defines the attenuation and delay that the channel incurs on subcarriers of 56 different frequencies. We expect that these different frequency electromagnetic waves will be affected uniquely by the physical medium they encounter [18]. Hence, their responses can be used to infer what was in the

signal path. More specifically, at any time  $t$  the CSI ( $H$ ) is dependent on the wireless link in the following manner [7]:

$$H(f, t) = H_s(f, t) + \sum_{k \in P} a_k(f, t)e^{\frac{-j2\pi d_k(0) + v_k t}{\lambda}} \quad (2)$$

where  $f$  is the carrier frequency,  $H_s(f, t)$  is the response of the static signal path,  $P$  is the total dynamic signal path,  $a_k$  is the attenuation on path  $k$ ,  $d_k$  is the path length from receiver to transmitter,  $v_k$  is the rate at which the length of the  $k^{th}$  path is changing, and  $\lambda$  is the signal wavelength.

### B. Three Device Architecture

As per Equation 1, CSI estimation requires a transmitter (Tx) to propagate a pilot signal to a receiver (Rx) and subsequent calculation of CSI. The organisation of Tx and Rx can be in two architectures: active or passive. In an active architecture, Tx will send a signal (usually a ping packet) to Rx, and the receiver will estimate the CSI using that packet. One tool available for this collection method is the Linux 802.11n CSI Tool [19] based on Intel 5300 Network Interface Card (NIC). Alternatively, a passive collection method involves three devices. Tx would broadcast packets to an Access Point (AP) as its intended recipient. Rx sniffs on this transmission and calculates CSI using the collected packets. This passive listening and CSI estimation is facilitated by the Nexmon CSI Extractor [6]. The Nexmon tool offers some advantages over Intel-based tool:

- Installable on Raspberry Pi's making it more portable;
- Outputs CSI on all 56 OFDM subcarriers as opposed to the Intel tool which provides 30 grouped subcarriers;
- The Nexmon tool is actively maintained as of writing (June 2020), allowing for more support.

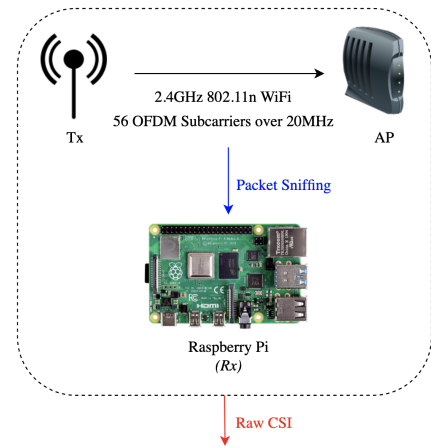


Fig. 1: Three Device Architecture

In a two device architecture there is a dedicated ongoing transmission between Tx and Rx, and Rx estimates CSI on inbound packets. Conversely, in a three device architecture the CSI estimation device (RX) sniffs on ambient transmissions between Tx and AP, hence there is no need for an additional dedicated transmitter. A three device architecture allows for

sensing given any wireless communication from the Tx. This allows for minimal hardware, computation, and power costs. Within the context of the COVID-19 pandemic, a cost effective solution with low installation overhead is desirable.

### C. Objective and Performance Metric

Having defined above a model for CSI and how it is affected by the channel, as well as an approach towards measuring it, we define our objective for this paper. We collect CSI for different occupancy scenarios in a given space and use CSI-based features to train a machine learning model. This model predicts how many occupants are in the space, whether we have exceeded the allowable occupancy limit. Occupancy limits in rooms are motivated by the enforcement of social distancing guidelines. For example, if people are to remain separated by 1.5m from each other, that means each person is allocated 4 square metres of space. Hence, the occupancy limit is calculated as the room area divided by 4, which *on average* assures that social distancing is being followed. This reasoning has motivated the enforcement of occupancy limits in public settings such as restaurants and bars in Australia. We perform such prediction in the practical scenario of an elevator, where the doors are opening/closing, patrons are talking and making small movements, and patrons carry mobile phones which are also introducing unwanted wireless interference.

To evaluate the success of CSI in distinguishing between occupancy levels, we will rely on two indicators. Firstly, we utilise a statistical tool to visualise the CSI for different occupancy levels. We group CSI amplitude into bins and evaluate that by a new metric defined as:

$$F_{|H(f,t)|}(x; f) = \sum_{t=1, x_{low} < |H(f,t)| \leq x_{up}}^T \frac{1}{T} \quad (3)$$

where  $F_{|H(f,t)|}$  denotes the Probability Mass Function (PMF) of  $|H(f,t)|$  for a given subcarrier  $f$  falling within the  $x$ th amplitude bin defined by the CSI amplitude values between  $x_{low}$  and  $x_{up}$ , which denote the lower and upper boundary of the  $x$ th bin, respectively. The statistical features of CSI amplitude can be visually examined by inspecting the PMF plots. Then, for a numeric performance metric, we use the classification accuracy that our machine learning model yields.

## IV. MACHINE LEARNING MODEL

In this section we introduce our framework for CSI based human counting for COVID-Safe spatial monitoring.

### A. Data Processing and System Flow

We use the aforementioned three device architecture for CSI collection, with Tx and Rx placed in opposite corners of the space and the AP placed adjacent to both. Tx sends ping packets towards the AP, to which Rx passively listens. Rx calculates the CSI for each received ping packet. The raw CSI is processed first with a Hampel filter to remove outliers, and then a low pass FIR filter to remove high frequency noise. These filters have been chosen since they are able to produce

outputs in real-time, which supports our end goal of real-time implementation. Existing work has shown a correlation between the shape of the CSI amplitude profile across OFDM subcarriers and objects in the channel, so we use features which characterise this shape [14].

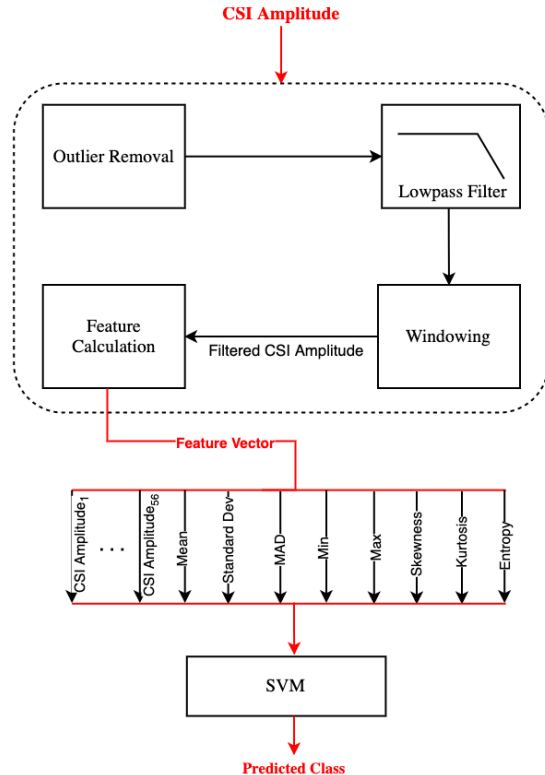


Fig. 2: Proposed Framework

### B. Feature Set

As mentioned, we propose that the CSI Amplitude profile across OFDM subcarriers is indicative of channel conditions. Hence, we produce the following set of 64 features:

- The first 56 features are the CSI amplitude on each of the 56 OFDM subcarriers.
- Mean of the CSI amplitudes across all subcarriers.
- Standard deviation of CSI Amplitude across subcarriers.
- Median Absolute Difference of CSI Amplitude across all subcarriers.
- Maximum CSI amplitude across the subcarriers.
- Minimum CSI amplitude across the subcarriers.
- Skewness, encompassing the asymmetric shape of the CSI subcarrier profile.
- Kurtosis of the CSI amplitude across 56 subcarriers, characterising how tail heavy the shape is.
- Entropy describes how much information is in our signal. We find the minimum  $H_{min}$  and maximum  $H_{max}$  values of our set of CSI amplitudes  $H$ , and create a set of 10 bins  $k$  which are in the linear space of  $[H_{min}, H_{max}]$ . We calculate the probability  $P_k$  of  $|H|$  being in each bin, by counting how many values in  $|H|$  are in bin  $k$ . Entropy is hence calculated as  $-\sum_{k=1}^{10} P_k \log_2 P_k$

These features are calculated for each training sample and the labelled dataset is used to train an SVM classifier in MATLAB. We optimise our choice of kernel polynomial degree to achieve high accuracies, and the resultant SVM can be fed data in real time to make predictions.

## V. EXPERIMENTAL SETUP

In this section we describe the experimental environment, and the hardware and software used. The experiment was conducted in an elevator as well as a generic indoor office environment. Their dimensions as well as key signal processing parameters are tabulated below:

TABLE I: Summary of Experimental Parameters

Parameter	Value
Elevator Dimensions	$2.5m \times 2m \times 2.5m$
Elevator COVID-Safe Occupancy	2 People
Office Dimensions	$10m \times 8m$
Office COVID-Safe Occupancy	5 People
Sampling Freq	1350Hz
Butterworth Cutoff Freq	5Hz
Hampel Filter Window Length	10
WiFi Centre Frequency	Channel 2 @ 2.417GHz

We instrumented the two test environments with three devices which act as a transmitter (Tx), a receiver (Rx) and an access point (AP). The Tx-Rx pair are positioned such that their line of sight covers the centre of each test environment. These setups are illustrated in Figure 3.

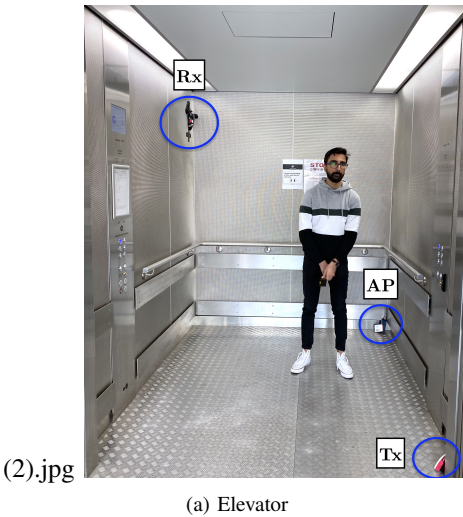


Fig. 3: Two Experimental Environments

All Raspberry Pi 4B's are equipped with a single internal antenna having 2dBi gain. Without losing generality, the devices are configured to communicate on channel 2 of the 2.4GHz band in accordance with the 802.11n WiFi standard. To collect CSI, we set up the Tx to send 1300 ping packets/sec to the AP. Rx passively listens to the ping packets sent by Tx and measures the CSI for the channel between Tx and Rx. Customised Nexmon CSI [6] extraction firmware for WiFi adaptor on Raspberry Pi was installed on the Rx. The Nexmon CSI extraction firmware captures CSI on all 56 OFDM subcarriers and pass it to MATLAB.

### A. Machine Learning

As proposed in Section IV we use an SVM approach to create decision boundaries that allow for inputs to be allocated to classes. For the first decision problem of counting occupants, we utilise a multi class SVM model using Error Correcting Output Codes (ECOC) [20] in the MATLAB Classification Learner Application. ECOC is an approach which breaks down the multi-class problem into multiple binary class problems and aggregates their results to estimate the true class of a sample [20]. The verification data is then used to assess the SVM classifier, producing a confusion matrix which demonstrates the performance of our classifier. For the second decision problem we aim to address, predicting COVID Safe Occupancy, we choose to train a *separate* binary classifier. Although we could use the previous multi-class classifier to predict of COVID-Safe occupancy has been exceeded, we note that a multi class ECOC approach is extremely computationally expensive relative to a single binary SVM. Hence, being mindful of the end goal of real-time implementation onto inexpensive hardware, we implement a simpler binary classifier to predict whether the COVID safe occupancy limit is violated. Each of these classifiers is predicated on the set of feature vectors outlined in Section IV. The overall training process is demonstrated in Figure 4. Our training/evaluation dataset comprises 80%/20% of the total data, and we use this to train SVM classifiers with 3 kernels: Linear, Quadratic and Cubic depending on the performance.

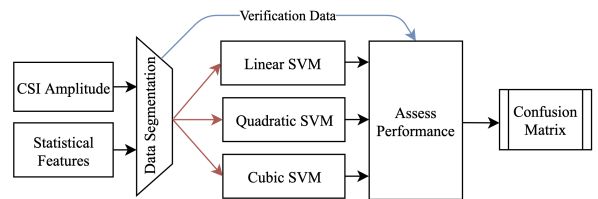


Fig. 4: Machine Learning Pipeline

## VI. EXPERIMENTAL RESULTS

In this section, we present results of our two experiments in the elevator and office.

### A. PMF For Different Occupancy Levels

First, we perform qualitative analysis of CSI for different occupancy levels. Without loss of generality, we only examine the PMF's for our data collected in the elevator.

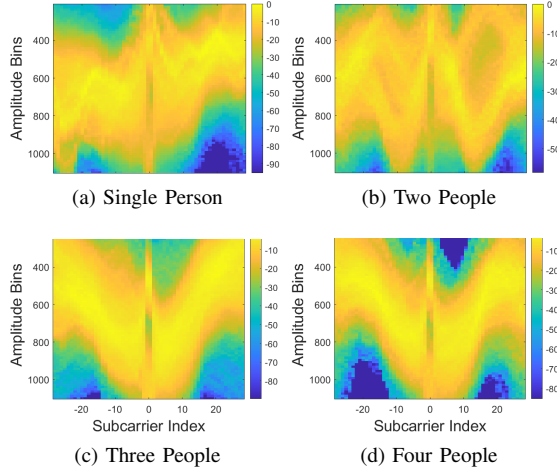


Fig. 5: PMF for different occupancy levels

In Figure 5 we present the PMF's for the 4 sets of CSI data in the elevator. In each case, the horizontal axis represents the *OFDM subcarrier index* and the vertical axis represents the *CSI Amplitude bins*. The color represents the distribution concentration of an amplitude bin for a subcarrier, with the deeper yellow tones implying higher concentration.

We observe a striking difference in the PMF for the first four occupancy levels. Visually, it is possible to observe a well-defined “W” shape for the PMF with an occupancy of two people, compared to the “V” shape PMF for when there is an occupancy of three and four people. We see that for each case, the scale of the amplitude bins are different. Additionally, there is some similarity between the PMF for three person occupancy and the PMF for four person occupancy. As we have introduced more occupants, we found that the influence on the CSI measurements became less pronounced as can be seen in Figure 5. Therefore, classification decisions are likely to be less accurate for an occupancy of greater than 4 people in this experimental environment. The detectable occupancy level will be dependent on the size of the sensing area, namely the elevator size and we were unable to experiment with more than 4 people due to the COVID-19 restrictions in place at the time of conducting the experiments. Finally, we note that for each scenario the different OFDM subcarriers display unique CSI amplitude distributions. This frequency selective behaviour motivates the use of the CSI Amplitudes on all OFDM subcarriers as 56 classification features.

### B. Counting Occupants

Next, we use the collected CSI to count the number of occupants inside each of our environments.

In Figure 6 the SVMs classify CSI measurements into occupancy classes, where class 0 corresponds to an empty room, class 1 corresponds to one occupant, class 2 is two occupants and so forth. We note that the confusion matrix has a higher dimension for the office, Figure 6b, since the larger environment allowed us to trial higher occupancy levels. The Confusion Matrix for the elevator represents a Cubic SVM,

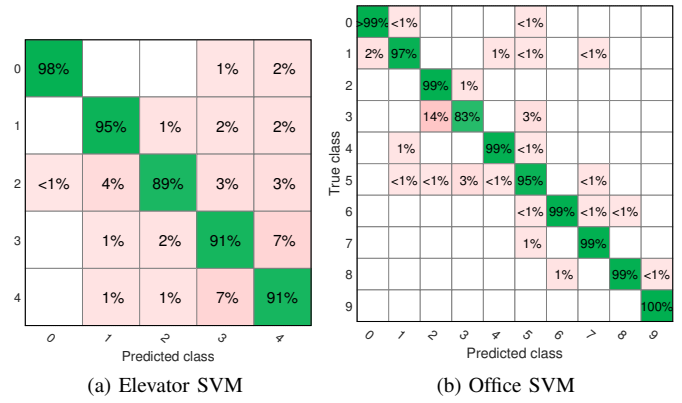


Fig. 6: Confusion Matrices for counting in each environment since the linear, quadratic and cubic kernels produced 81%, 89% and 92% prediction accuracies, respectively. It is important to note that cubic SVM classifier takes substantially more time to train, however in our opinion it might be an acceptable trade-off for the improvement in accuracy. Conversely, the Linear SVM for the larger office environment achieved an accuracy in excess of 95%, and hence we did not deem a more expensive cubic kernel necessary.

For the elevator, We observe the highest prediction accuracies at lower occupancy levels, with our true positive rate at 98% for an empty channel. As expected, the classifiers true positive rate decreases for higher occupancy levels as there is less variation in PMF between higher occupancy levels. However, despite the PMF's for four-person occupancy and three-person being visually similar, the SVM classifier had a 92% accuracy. Importantly, only 7% of the class 4 CSI samples are incorrectly classified as class 3 by the cubic SVM classifier. We postulate that this is due to the novel features we use, and the ability of our cubic SVM classifier to compensate for the loss of sensitivity of CSI in congested area. In contrast with the elevator where we saw a drop-off in accuracy for higher occupancy's, we see a steadily high accuracy across the leading diagonal of the confusion matrix in Figure 6b. This indicates that our system scales well to larger environments. This can be understood with reference to Section VI-A where we saw smaller difference in the PMF's for larger occupancy levels in the small environment. It is worth noting that more than 10% samples of 2 occupants were classified as 3, whereas for all other occupancy cases only a negligible number of incorrect predictions were made. It should also be noted that for higher occupancy levels the counting accuracy did not show signs of saturation like it did in the elevator. This result shows that saturation might be related more so to the dimensions and size of the room.

### C. Predicting COVID-Safe Occupancy

We are motivated to outperform existing WiFi crowd-counting works in a COVID context, and in this section we show that a simple binary classifier offers comparable prediction accuracy with a lower complexity that would allow for light weight implementation on embedded devices.

Our binary SVM classifier achieved an accuracy of 97% in determining whether the 2-person COVID-Safe occupancy limit in the elevator was breached. In the Office environment, the Binary SVM is able to make the same COVID-safe decision to an accuracy of 92%. In the previous section it was demonstrated that the proposed multi-class SVM classifier can count occupancy levels. Given the COVID Safe occupancy allowance of 2 people, we could hypothetically use the multi-class classifier to predict whether the safe limit has been exceeded. For comparison with the binary SVM, we demonstrate how the Elevator counting SVM could be used for COVID-safe decision making. Within this multi-class SVM model, classes zero, one and two could be clustered into a single class for occupancy  $\leq 2$  people. The second class is then the grouping of classes three and four. We analyse the prediction accuracy around the boundary of our two clustered classes, 2 occupants, to determine the performance of our multi-class model for binary classification. From Figure 6a, we observe that 2 person occupancy is incorrectly classified as 3 people or 4 people 3% of the time. Additionally, classes 3 and 4 are incorrectly classified into cluster 1 5% of the time. In effect this means our multi-class classifier will make an incorrect COVID-Safe occupancy decision *at least* 8% of the time. Hence, using a dedicated binary classifier offers similar or better accuracy for the COVID-safe decision as using the counting classifier and clustering classes. As discussed in Section V, multi-class SVM's are an aggregation of multiple binary SVM's, and hence they will always be considerably more expensive. The simplicity of our binary classification model allows for real-time implementation on resource constrained devices with low computational capabilities.

Referring again to Figure 6b, the only major misclassification for the Office SVM is between class 3 and class 2. Since both class 2 and class 3 are below the occupancy limit of 5, this misclassification is inconsequential to our COVID-safe decision problem. Hence, for the office it would be slightly more accurate to use the multi-class SVM and aggregate classes to subsequently predict if the occupancy is unsafe. However, in line with the main motivation of this paper, we note that the binary SVM is significantly less computationally expensive for a small tradeoff in accuracy. With an ECOC scheme as outlined in Section V, the 10-class counting SVM will be comprised of 45 binary SVM's. Accounting for variance in the support vector length, the multi-class SVM is close to  $45 \times$  more computationally expensive.

## VII. CONCLUDING REMARKS

This paper presented a privacy-preserving, low-cost method that can be used to enforce social distancing adherence and raise an alarm when the guidelines are not observed. Our proposed method does not rely on users possessing any devices, and leverages ubiquitous WiFi which makes it cost effective. The proposed system exploits frequency selective characteristics of CSI amplitude to determine the number of people in a given area. This is done through the use of a novel feature set including smoothed CSI amplitude and

statistical parameters. The system's performance was evaluated empirically to determine the number of occupants in an elevator and a commercial office, where the adherence to social distancing is crucial. The classification model was able to count the number of occupants in these environments to accuracies of 92% and 97% respectively. Motivated by the COVID-19 pandemic and with deployment onto lightweight portable devices in mind, this paper shows the utility of simple Binary classifiers for predicting whether the COVID-safe occupancy limit is breached. This approach offers similar accuracy outcomes to the well studied counting method, at a fraction of the computational cost.

## REFERENCES

- [1] A. G. D. of Health, "Physical distancing for coronavirus (covid-19)," May 2020. [Online]. Available: <https://www.health.gov.au/news/health-alerts/novel-coronavirus-2019-ncov-health-alert/how-to-protect-yourself-and-others-from-coronavirus-covid-19/physical-distancing-for-coronavirus-covid-19>
- [2] Airista, "Social distancing and contact tracing - rtl solutions," <https://www.airistaflow.com/industries/government/social-distancing-and-contact-tracing/>, 2020.
- [3] Sonarax, "Social distancing keeper," <https://www.sonarax.com/social-distancing-keeper>, 2020.
- [4] Skyfii, "Occupancynow: Automated occupancy and social distancing management toolkit," <https://skyfii.io/occupancynow>, 2020.
- [5] National University of Singapore, "Singapore spacer," <https://sleepcoglab.wixsite.com/singaporespacer>, 2020.
- [6] F. Gringoli, M. Schulz, J. Link, and M. Hollick, "Free your csi: A channel state information extraction platform for modern wi-fi chipsets," 10 2019, pp. 21–28.
- [7] Y. Ma, G. Zhou, and S. Wang, "Wifi sensing with channel state information: A survey," *ACM Computing Surveys*, vol. 52, pp. 1–36, 06 2019.
- [8] H. Abdelnasser, M. Youssef, and K. A. Harras, "Wigest: A ubiquitous wifi-based gesture recognition system," in *2015 INFOCOM*, 2015, pp. 1472–1480.
- [9] J. Lv, D. Man, W. Yang, L. Gong, X. Du, and M. Yu, "Robust device-free intrusion detection using physical layer information of wifi signals," *Applied Sciences*, vol. 9, p. 175, 01 2019.
- [10] S. Yousefi, H. Narui, S. Dayal, S. Ermon, and S. Valaee, "A Survey on Behavior Recognition Using WiFi Channel State Information," *IEEE Commun. Mag.*, vol. 55, no. 10, pp. 98–104, 2017.
- [11] Y. Zeng, P. H. Pathak, and P. Mohapatra, "Wiwho: Wifi-based person identification in smart spaces," in *2016 IPSN*, 2016, pp. 1–12.
- [12] F. Li, M. A. A. Al-qaness, Y. Zhang, B. Zhao, and X. Luan, "A robust and device-free system for the recognition and classification of elderly activities," *Sensors*, vol. 16, p. 2043, 12 2016.
- [13] C.-x. WU, H. SU, and K. YU, "A wireless signal denoising model for human activity recognition," *DEStech Transactions on Computer Science and Engineering*, 04 2017.
- [14] C. Wang, J. Liu, Y. Chen, H. Liu, and Y. Wang, "Towards in-baggage suspicious object detection using commodity wifi," in *2018 IEEE CNS*, 2018, pp. 1–9.
- [15] F. Wang, J. Han, F. Lin, and K. Ren, "Wipin: Operation-free passive person identification using wi-fi signals," 12 2019, pp. 1–6.
- [16] S. Liu, Y. Zhao, F. Xue, B. Chen, and X. Chen, "Deepcount: Crowd counting with wifi via deep learning," 03 2019.
- [17] Z. Wang, K. Jiang, Y. Hou, W. Dou, C. Zhang, Z. Huang, and Y. Guo, "A survey on human behavior recognition using channel state information," *IEEE Access*, vol. 7, pp. 1–1, 10 2019.
- [18] A. Sharma, D. Mishra, T. Zia, and A. Seneviratne, "A novel approach to channel profiling using the frequency selectiveness of WiFi CSI samples," in *IEEE GLOBECOM*, 2020, pp. 1–6.
- [19] D. Halperin, W. Hu, A. Sheth, and D. Wetherall, "Tool release: Gathering 802.11n traces with channel state information," *Computer Communication Review*, vol. 41, p. 53, 01 2011.
- [20] Northeastern-University, "Ecoc." [Online]. Available: [http://www.ccs.neu.edu/home/vip/teach/MLcourse/4\\_boosting/lecture\\_notes/ecoc/ecoc.pdf](http://www.ccs.neu.edu/home/vip/teach/MLcourse/4_boosting/lecture_notes/ecoc/ecoc.pdf)